

Conference Paper

Numerical Analysis of Load Distribution in Joint Lines with Punched Metal Plate Fasteners

Lucas Paiva, Manuel Braz-Cesar, and Miguel Paula

Polytechnic Institute of Bragança

Abstract

Wood trusses with traditional bolted or nailed connections are generally modeled as pinned joints, and the forces on the wooden members are directly transmitted to the connections by shear plane contact. Other methodologies recommend that the analysis should be done more rigorously, taking into account the wood behavior and the evaluation of stress distribution within the connection area. There is a wide range of related data to pin-type connections, but the mechanical analysis of punched metal plate fasteners (nail plates) is still under developed. Nail plate connections are capable of transfer moments, therefore, appropriated modeling should be applied. The present paper compares two methodologies for the stress distribution in the rupture lines of nail plates, using an analytical approach and a numerical method with the commercial software Midas/Gen. The results show a quantitative parity for the proposed analytical model in the case of a single joint line, but the stresses diverge in both methods for zones that presents more than one joint line.

Keywords: Timber, nail plate, structural analysis

Corresponding Author:

Lucas Paiva
a39542@alunos.ipb.pt

Received: 26 November 2019

Accepted: 13 May 2020

Published: 2 June 2020

Publishing services provided by
Knowledge E

© Lucas Paiva et al. This article is distributed under the terms of the [Creative Commons Attribution License](#), which permits unrestricted use and redistribution provided that the original author and source are credited.

Selection and Peer-review under the responsibility of the ICEUBI2019 Conference Committee.

1. Introduction

Wood is probably the oldest building material, dating from prehistory, where fallen trees were used as bridges to new lands. Few materials have as many structural applications as wood, and in addition it carries sustainability concepts as a low-embedded energy and recyclable material. However, the development of wood in the structural field is linked to the knowledge of connections properties and to the analysis methods used to evaluate load distributions and design parameters. The motivation of study on timber connections comes from the unavailability of wood pieces that are compatible with the design requirements, either by structural geometry or by the high resistance capacity [1, 2].

Among all types of mechanical connectors, punched metal plate fasteners (nail plates) are the most efficient. These plates are commonly used in the manufacture of prefabricated wooden trusses, and their low cost and easy production are the biggest

 OPEN ACCESS

advantages over other types of mechanical joints. The shear connection mobilizes a large contact area by the embedded teeth, which justifies the high efficiency compared to e.g. regular pin-type connections [3].

Nail plates are galvanized steel plates with thicknesses between 1–4 mm and with teeth “punched out” of the plate in a perpendicular direction with a size range of 4–10 mm. These plates are fixed on each side of the wood by presses and, for this reason, the production is made mostly in industry sites. Figure 1 illustrates a model of common rectangular nail plate shape used in wooden trusses.

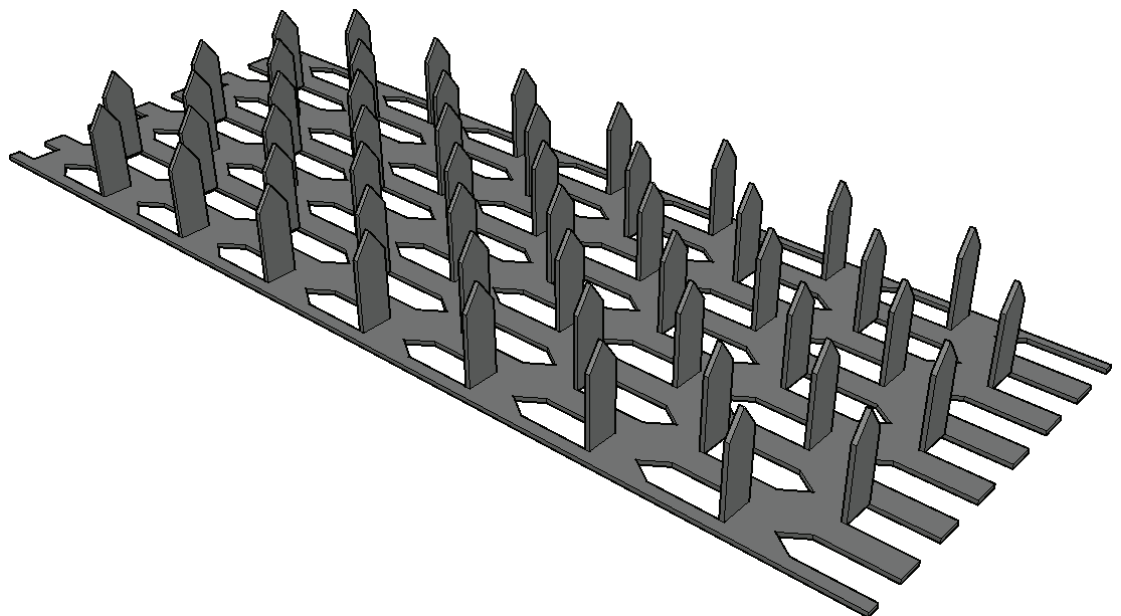


Figure 1: rectangular nail plate design

Nail plates are widely used in North America, Europe and United Kingdom since its invention in 1952. The nail plate industry is a multimillionaire branch of civil construction and these connections are used in more than 90% of house roofs in the United States. Interestingly, there is not a lot of research about the design and modelling, probably because of the commercial sensitivity around truss industries [4, 5].

Unlike most wood truss connections, nail plates are capable of transferring bending moments. Thus, current simplifications in wood trusses, modelled as hinges, need to be reformulated to better predict the truss behaviour in terms of load distribution and deflections. The main reference to the connection design is the European standard EN 1995-1-1:2004 (EC5) which brings the ultimate limit state (ULS) equations, but present scarce information about the mechanical modelling. The present paper aims to contribute to the current research stage and present two approaches to load distribution in joint lines.

The two ULS equations from EC5 are based in the stress flow in nail plates. The force is initially transferred from the timber to the nails by an anchorage area, then from the nails to the steel plate. In the joint line, the net-cross-section transfer the forces to the other side of the plate and finally to the other side of the joint. Thus, two failure modes are identified: the capacity of the anchorage area to resist the distributed forces and the maximum load supported by the net-cross-section. Therefore, the design steps of a nail plate connection consist in determining the forces applied in the anchorage area and at the cross section.

The next section briefly reviews the state-of-the-art in nail plate modelling.

2. Literature Review

Misra and Esmay [6] conducted one of the first analytical proposals to evaluate the load distributions within the plate. The model considered only one plate geometry and it was assumed that the behaviour of timber-plate combination would be linear-elastic. The theoretical curves evaluated correctly the maximum load capacity in the cases when the failure mode was splitting. However, the load-slip curve did not adjust the experimental curve. One reported reason for data divergence was the linear-elastic approximation and the rigid-member consideration about the plate behaviour.

A pioneer finite element method (FEM) was present by Foschi [7] and many subsequent researches are based on the following considerations. The 2D model assumed that the timberplate interface was rigid, connected by non-linear springs. The stiffness of each spring, that simulated each “tooth” in the plate is evaluated according to mechanical and geometric plate properties. Load-slip was experimentally determined as:

$$P = (m_0 + m_1 |\Delta|) (1 - e^{-k|\Delta|/m_0}) \quad (1)$$

where P is load on the joint, Δ is joint slip, k is initial slope of the curve, m_1 is asymptotic slope of the curve and m_0 is intersection of the asymptotic slope with the load axis. Foschi's proposition successfully predicts max-load and slip curves, but the analysis was restricted to 2D failure modes, thereby tooth withdrawal and other out-of-plane modes could not be predicted.

Lau [8] studied the heel joints shown in Figure 2. The red dots indicate where slip was measured, and was observed that the plate positioning can create a high friction force in the wedge section, and therefore changing the failure mode. In the cases where the major plate axis was oriented in the same direction to the tension member

— (a) — the failure mode was tooth withdrawal. When the major axis was oriented to the compression member — (b) — failure mode was majority plate buckling. Two plate sizes were tested for the same configurations and have shown that the plate size is a significant factor in the plate buckling failure, but had low impact in the tooth withdrawal.

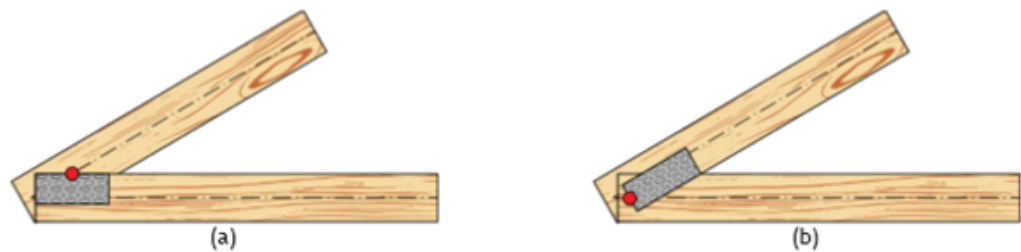


Figure 2: Heel joint configuration for two plate positions Source: [8]

Cramer et al. [9] approached the nail plate joint problem and classified the joint as a threepart system: wood, metal plate and wood-tooth interface. Each tooth was assigned with three interdependent non-linear springs to simulate two translations and one rotation component, following Foschi's parameters. The load was applied by steps with small increments, considering that in each interval, the behaviour was linear. The linear results were then combined and the curves adapted well to the experimental results. The work contributed with an extension of Foschi's proposal, but still in the 2D plane analysis.

3. A Heel Joint Model

As already stated, there are two EC5 equations that must be satisfied in terms of ultimate state that comes with the load distribution in two stages: the distributed forces applied at the anchorage area and the forces at the joint lines. The first model that transfers the loads from the timber to the geometric center in the anchorage area is well documented on the third part of the French Standard DTU 31.3. The results given by the structural model are the loads acting in the anchorage area (Figure 4) and allow a straight forward anchorage area verification, therefore it will not be detailed here. This paper intends to provide further information in the net-cross-section verification, by the analysis of the joint illustrated in Figure 3:

The heel joint studied is composed by two timber pieces and a wedge. The top timber contact was modelled without the friction force in the wedge contact, thus the top timber loads are integrally transmitted by the timber axis. The objective is to transfer the loads applied at the geometric center of each region to the joint lines (red, green and blue), as shown in Figure 4. The problem is pointedly undetermined, as each line

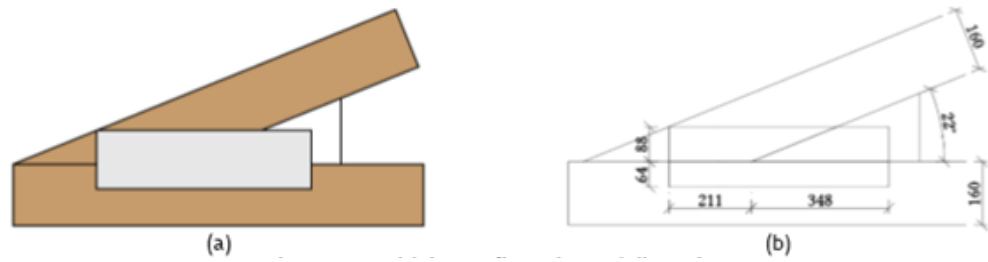


Figure 3: Heel joint configuration and dimensions.

requires three distinct force values that need to be solved simultaneously. Besides, there is no initial boundary conditions.

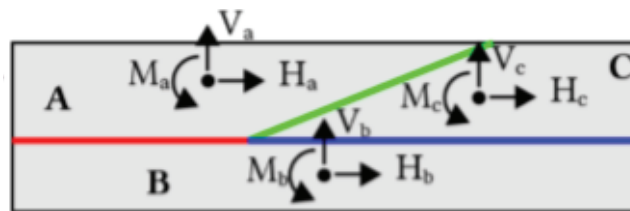


Figure 4: Loads applied at the barycentre of each region.

In the following, two approaches are proposed to solve the load distribution to the joint lines.

4. Model 1 - Analytical Solution

More than a mere statically indeterminate structural problem, the solution of a nail plate comes with the understating of how the plate and joint behaves, and how to summarize this knowledge to formulate boundary conditions. The analytical solution here proposed starts with the condition in which all the lines are simultaneously deforming, configuring the load mode in which the forces are applied at the same instant and the small deformation principle is valid. This allows that one region can be calculated independently and then the forces can be transferred to adjacent regions. This is helpful in the cases where the region is delimited by only one joint line, otherwise the problem remains indeterminate. By inspection, region B can be separated and the distribution will be as follows:

Table 1 summarizes the loads in the region's barycentre, indicating positive values in green and negative values in red:

$$\sigma_{m,b} = \frac{4 \cdot (H_b \cdot e - M_b)}{\ell} = \frac{4 \cdot (26,2 \cdot 0,0345 - 0,20)}{0,559^2} = 9 \text{ kN/m} \quad (2)$$



Figure 5: region B isolated analysis by the analytical model

TABLE 1: Numerical results for the barycenter

Loads	V	H	M
Regioes	[kN]	[kN]	[kN.m]
A	7,67	-28,20	-0,70
B	-6,34	26,20	-0,20
C	-1,51	2,22	-0,22

$$\sigma_b = \frac{V_b}{\ell} 11,3 \text{ kN/m} \tag{3}$$

$$\tau_b = \frac{H_b}{\ell} 46,9 \text{ kN/m} \tag{4}$$

where e is the horizontal load eccentricity and ℓ is the line length, as shown in Figure 5b. The principle of superposition was applied to transport the loads from the region's barycentre to the joint line center. Eccentricates were evaluated (horizontal force) and the moment was converted to a moment arm force to better visualize the numerical proportions between loads. As all the joint lines were assumed to deform proportionally and the region B shares adjacent lines with both A (red) and C (blue) regions, the values obtained could be either transferred to region A or C in order to evaluate the inclined line (green).

The load distribution results are summarized in Table 2:

TABLE 2: Summary of the load distribution by the analytical model

	V	H	M
Joit line	[kN/m]	[kN/m]	[kN.m]
Horizontal	-11,30	46,90	9,00
Inclined	-14,74	78,36	-23,18

5. Model 2 - Numerical Approach

The analytical model was presented to study simple cases and to understand how to formulate boundary conditions according to the nail plate behaviour concepts. The case

in which all the lines are mutually deforming, and therefore possible to transfer forces from adjacent plates regardless of its order could be verified, unless each region, with its own loads, are not verified. A second model is then required to verify each region separately, as illustrated in Figure 6:

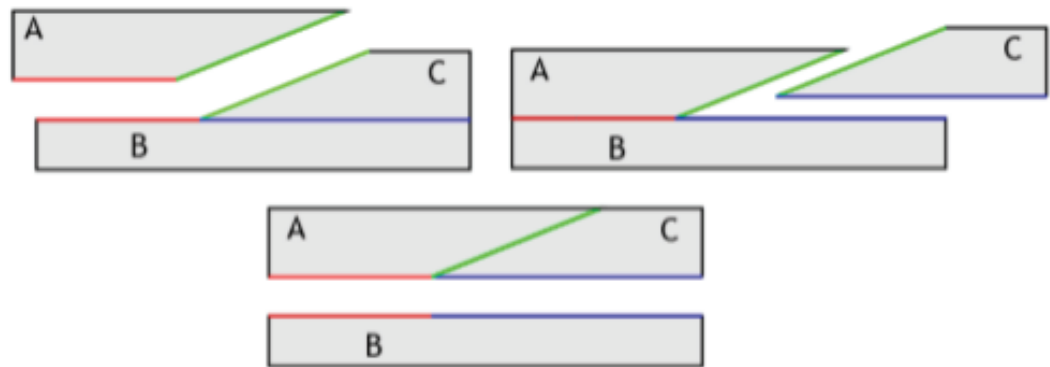


Figure 6: Region withdrawal modes

With a numerical tool, in this case the Midas/Gen software, it is possible to solve regions that have more than one joint line with the described process, which is based on Foschi [7] and Cramer [9] proposals. Initially, the line is divided by a finite integer number and to each new node, a set of springs are addressed. The springs will evaluate the slip in the nodes, and by multiplying by its stiffness, it is possible to extract a discrete value, that represents the distributed force in each node. There are two springs per node, to account for horizontal and vertical deflections. The line behaviour is considered rigid, therefore there will be no relative rotation between two adjacent nodes. The spring stiffness is calculated based on the German Standard DIN 1052:2008-12, at section 2.3.4.1 that describes both horizontal and vertical springs based on the slip modulus k_{ser} , parameter given by the plate manufacturer manual:

$$K_u = \frac{2}{3} \cdot \frac{k_{ser}}{\gamma_m} \tag{5}$$

$$K_x = K_y = 2 \cdot K_u \cdot A_{anc} \tag{6}$$

Where γ_m is the partial factor for material properties and A_{anc} is the anchorage area for the analysed region. The rigid behaviour for the joint line is approximated using a rigid link type member (blue). A rigid link applies geometric constraints to a group of nodes (slave nodes) in relation to a master node (barycentre where the loads from the anchorage area are applied in each region). The spring stiffness is defined by a spring element (yellow) that has both k_x and k_y properties. Figure 7 illustrates how the region B would be designed by the elements previously described:

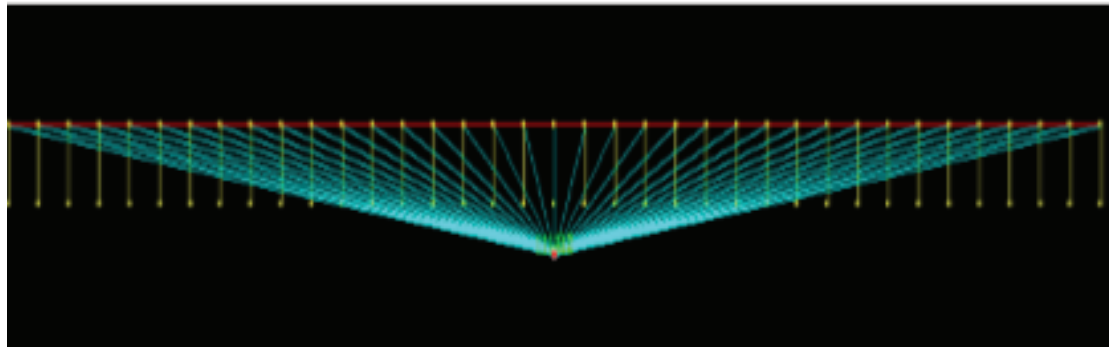


Figure 7: Region B elements in Midas/Gen software

In order to directly compare results from both models, the analytical model, which gives a discrete force value, a weighted average can be obtained by distributing each node force by its influence area. The discretization factor must be evaluated by steps until it normalizes the results. For this region example, the finite element adopted has 15mm (36 elements and 37 nodes).

Using the same approach, regions A and C can be modelled as illustrated in Figure 8:



Figure 8: Region withdrawal modes

Table 3 summarizes the spring stiffness used in each region:

TABLE 3: Spring stiffness used for each region in the numerical model

Region	$k_x = k_y$ [kN/cm]
A	898
B	1181
C	577

6. Results and Discussion

Comparing both analytical and numeric solutions given in Figure 9 for the initial proposed region B, two observations should be highlighted. Firstly, the analytical model proved to be numerically acceptable taking into account the load distribution by the superposition principle, although its static limitation based on a single joint line. Secondly, the plastic consideration (given by a linear load-slip diagram) in the analytical

model diverges from the plastic deformation shown in the numerical model. This could be explained as a limitation in the analytical model, in which only a balance of forces is conducted without defining a stress-strain relationship. The Numerical model provides a more precise analysis, first evaluating the deformation parameter and after the node forces by the stiffness matrix method.

Because of its rigid nature and the linear-elastic spring type, the line rotation by its center point gives, at each adjacent node, a slip increment which is converted in a linear increment of force, generating the expected plastic behaviour. As the geometric center of the triangular bending moment (plastic) it is further located from the line's center as in the rectangular (elastic), a bigger bending moment value is expected in the numerical model.

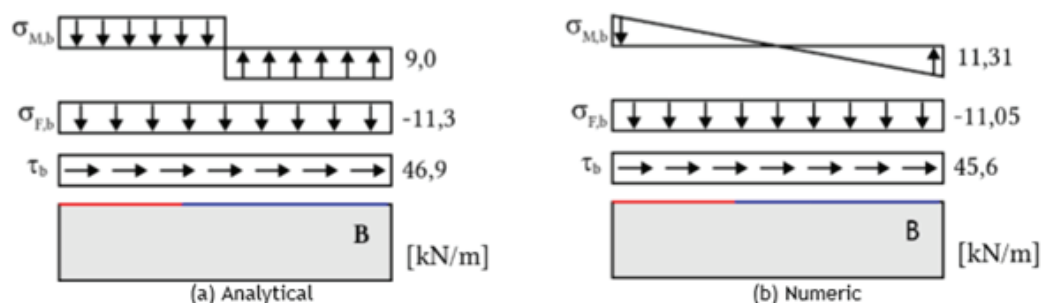


Figure 9: Region B comparison by the two models

As the joint lines in the numeric model are evaluated separately, there is no need to a qualitative analysis of the other regions. The results from the numeric model in the region B were applied as reactions in the adjacent regions to obtain the load distribution at the inclined line level. Because there is no interdependence between adjacent lines in the numerical model, two possible modes were evaluated: first transferring to region B and first transferring to region C. Table 4 summarizes the load distribution results described:

TABLE 4: Summary of load distribution results from Analytical and Numeric methods

Load Distribution		V	H	M
Method	Joint line	[kN/m]	[kN/m]	[kN.m]
Analytic	Horizontal	-11,30	46,90	9,00
	Inclined	-14,74	78,36	-23,18
Numerical	Horizontal	-11,05	45,60	11,30
	Inclined (A)	16,78	80,24	39,18
	Inclined (C)	-16,58	77,98	-20,84

The load at the inclined line varied in both qualitative and quantitative value. Due to the high variability in the results for each line, the ultimate states analysis should be taken upon the most critical case. However, it is important to precisely define all the possible failure modes to avoid design the nail plate based on high fictitious forces at the joint lines.

7. Conclusions

Both models 1 (Analytical) and 2 (Numerical) provide approximate results when dealing with the isostatic case, but differ according to the criterion of hyperstatic analysis. Consideration of plastic behaviour is not verified in the numerical method, where the force distribution results suggested an elastic relationship between stress and strain.

The simplification adopted, that the rupture lines are interdependent from the point of view of deformation, provides a result for only one rupture mode. In the actual mechanical behaviour of a joint line, the joint lines may indeed present other failure modes, and therefore for cases that there is not a single joint line per region, a numerical approach is required.

The divergence of the models suggests the need to implement other calculation approaches and formulate new boundary conditions, besides experimental tests to validate the ideal model.

References

- [1] Mamlouk, M.S. and Zaniewski, j.p. (2010). *Materials for Civil and Construction Engineers*. Pearson.
- [2] Porteous, J. and Kermani, A. (2007). *Structural Timber Design to Eurocode 5*. Macmillan International Higher Education.
- [3] Callahan, E.E. and Dinsmore, P.W. (1993) *Metal Plate Connected Wood Truss Handbook: A Comprehensive Guide to the Design and Use of Metal Plate Connected Wood Trusses in Construction Today*. Wood Truss Council of America.
- [4] Gupta, R., Vatovec, M., Miller, T.H., et al. (1996). Metal-plate-connected wood joints: a literature review. *Forest Research Laboratory Oregon State University*.
- [5] Gebremedhin K.G. and Crovella P.L. (1991). Load distribution in metal plate connectors of tension joints in wood trusses. *Transactions of the ASAE* vol. 34, issue 1, pp. 281–287.

- [6] Misra R.D. and Esmay M.L. (1966). Stress distribution in the punched metal plate of a timber joint. *Transactions of the ASAE* vol. 9, issue 6, pp. 839–842.
- [7] Foschi, R.O. (1977). Analysis of wood diaphragms and trusses. Part II: Truss-plate connections. *Canadian Journal of Civil Engineering*, vol. 4, issue 3, pp. 353–362.
- [8] Lau, P. W.C. (1987). Factors affecting the behaviour and modelling of toothed metal-plate joints. *Canadian Journal of Civil Engineering*, vol 14, issue 2, pp. 183–195.
- [9] Cramer, S.M., Shrestha, D., and Fohrell, W.B. (1990). Theoretical consideration of metal-plate connected wood-splice joints. *Journal of Structural Engineering*, vol. 116, issue 2, pp. 3458– 3474.
- [10] EN 1995-1-1. Eurocode 5: Design of timber structures (2004). *Part 1-1: General – Common rules and rules for buildings*. European Committee for Standardization.
- [11] NF DTU 31.3. (2012). *Timber structures connected with metal plate fasteners or gussets –Part 3: Design requirements*. Association Française de Normalisation.
- [12] DIN 1052:2008-12. (2008). *Nagelplattenbinder nach*. Nagelplattenprodukte.